Birefringence, Deformation, and Scattering of Wormlike Macromolecules under an External Agent. Steady-State Properties in an Electric Field

H. E. Pérez Sánchez, J. García de la Torre, and F. G. Díaz Baños*

Departamento de Química Física, Universidad de Murcia, 30071 Murcia, Spain

Received: February 13, 2003; In Final Form: August 15, 2003

In this paper, we study the steady-state birefringence, deformation, and scattering of wormlike macromolecules under the influence of an electric field. We use a model of $N + 1$ pointlike elements whose connectors define N axially symmetric subunits. The model is able to describe some properties of segmentally flexible and wormlike macromolecules depending on the choice of N. We use the Monte Carlo computer simulation technique to characterize the effect of the electric field on the orientation and deformation of molecules with permanent and induced dipoles. Using this technique, we study the effect of the field in different models with the same flexibility (defined as $\langle s^2\rangle_0/\langle s^2\rangle_{0,str}$). Orientation is studied through changes in birefringence and deformation through changes in the gyration tensor of the molecule. When the behavior of a broken rod (typical case of segmental flexibility) and a wormlike chain is compared, the differences are generally quantitative although significant enough to be used to obtain information about the internal structure of a macromolecule.

Introduction

A macromolecular solution becomes birefringent or dichroic when an external agent orients the molecules of solute. Such is the case when an electric field is applied and when the solution is submitted to shear, elongational, or other types of flow. In some circumstances, a magnetic field yields the same results. The essential aspects of the techniques based on these properties have been described in several monographs.[1,2] In addition to undergoing a change in the orientation, the macromolecule suffers certain effects, such as deformation, that can be measured and related to its structure, flexibility, and other internal characteristics.

The study of macromolecular solutions under the influence of an electric field and, in general, of any external agent, presents two different aspects, one involving the properties of the macromolecule in its steady state (when that agent has been applied for a sufficiently long time) and the other the way in which the properties change when the agent is switched on or off. In this paper, we pay attention to the steady-state properties in an electric field. The birefringence and, to a lesser extent, the deformation or scattering, of macromolecules under external agents such as fields or flows is well understood when the macromolecule behaves as a completely rigid particle.[3−7] However, many macromolecules, usually grouped under the name of semiflexible molecules, present a certain degree of flexibility in solution. A rigorous and general description of the electrooptics of these macromolecules is very difficult, since their conformational flexibility, interaction with the electric field, and internal mobility are interrelated.

Different models have been developed to describe the flexibility of these macromolecules and to study their electrooptics (and other properties). Among them, two extreme and relatively simple models have become very popular: segmental and wormlike flexibility.

In the first, macromolecules are modeled by few rigid subunits or domains, joined by more or less flexible hinges or joints. A typical case is that of broken-rod macromolecules with two rodlike arms, a model that has been used to study the myosin rod[8,9] or some especially prepared synthetic polypeptides.[10,11] Whole myosin[8,12] and immunoglobulins[13] are more complex examples, with more subunits and joints. Studies of the electrooptic properties of this type of molecule have recently been published by this group for steady-state[14] and transient[15,16] properties.

In wormlike macromolecules, flexibility is not localized at a single or even in a few joints but distributed along the macromolecular chain. Macromolecules with a helical structure are usually considered to present this kind of flexibility and the most paradigmatic example is probably DNA.[17,18]

Of course most real semiflexible molecules present a mixture of both types of flexibility, although one may be more relevant defining its characteristics. RNA is a good example.[19] Although structural differences between wormlike and segmentally flexible molecules must be substantial, experimental results can be interpreted using different models with plausible results. Good illustrative examples are models that treat DNA as a broken rod ("hinged bent rod")[20] and those that model it with 3 and 10 beads.[21,22]

The interaction of macromolecules with an external agent is usually characterized in terms of the birefringence or dichroism induced in the macromolecular solution by the orientation of the subunits. Furthermore, a frequent simplifying assumption is to make the external field very weak, so that the perturbation in the conformational statistics of the macromolecule is very small. Under an electric field, the steady-state, field-on electrooptic properties are then given by Kerr's Law.[1] The cases of moderate or even rather high fields present difficulties both for the realization of experiments as well as in the formulation of theories and are seldom considered. However, it is precisely in these strong fields where the interplay between field effects and

* To whom correspondence should be addressed. E-mail: fgb@um.es.

10.1021/jp0302111 CCC: $25.00
Published on Web 11/01/2003

the limited flexibility of the macromolecule becomes more evident, yielding important information about the structure and flexibility itself.

While the theoretical study of the behavior of macromolecules under external forces or fields of arbitrary strength presents notable difficulties, it is quite simple to predict such behavior using simulation. Our group has previously contributed to the study of steady-state birefringence of macromolecular solutions for different cases of flexibility, including rigid bent-rod macromolecules,[23] totally flexible polymers,[24] and segmentally flexible macromolecules with two subunits in an arbitrary field.[14,25] In this paper, we study wormlike flexibility and pay special attention to its comparison with segmental flexibility.

Although birefringence (and similarly dichroism) is the most frequently studied property in this context, another important effect of the external agent is to deform the macromolecule, altering its conformational statistics, and therefore changing its overall dimensions. Scattering of light or other electromagnetic radiation is capable of monitoring such changes because changes in scattering intensity reflect change in the distribution of conformations. Indeed, the technique of electric field light scattering has been experimentally investigated,[26,27] although its use is not widespread. Light scattering in flows is also an interesting possibility.[28,29] In this paper, we use the theoretical formalism developed in a previous work[14] for describing deformation and scattering intensities and apply it to semiflexible macromolecules. We also use the relationships between the overall particle deformation measured by scattering and the orientation of segments measured by electric birefringence.

As mentioned above, the efficiency of an external field to deform the semiflexible macromolecule or orient its subunits depends both on the interaction of the field and the molecule (field strength and type of dipole) and the type and degree of flexibility. Therefore, the study of such effects as a function of field strength should provide valuable information regarding macromolecular structure. To illustrate this hypothesis with numerical results, we study the properties (electric birefringence or dichroism, as well as deformation and scattering) of different models under the influence of an electric field. When one flexible region alone is defined inside the macromolecule, this segmental flexibility is well described by a two-subunit model. This is the case for a variety of biological systems.[14,25,30,31] Ideally, the description of wormlike flexibility would need a quasi-infinite number of subunits. However, the use of simulation to study this type of flexibility requires a model made up of a discrete number of subunits, the exact number of which will be a compromise between computational cost and accuracy.

The analysis of the experimental data from the published literature illustrates the interest and usefulness of this kind of modeling for semiflexible macromolecules under the influence of an electric field of any intensity. We shall mention some examples. The electric field orientation of DNA in solution has been the subject of several studies, that is, dependence of steady-state electric birefringence on field strength,[32] calculation of the optical factor and the electric polarizability as a function of molecular weight,[33] or the study of the influence of the orientation of the molecular weight dependence of the free solution mobility of this molecule.[34] The internal flexibility of filaments of myosin II has been investigated studying its dependence both on Mg^{2+} concentration and on the state of phosphorylation.[35] Other examples of molecules which have been studied through their steady-state electrooptical properties are acetylcholinesterase[36] and polyciacetylenes.[37] Finally, another factor of interest is the possibility of extending some experiments, developed at low fields (in the region where the Kerr law is obeyed),[33,37,38] to higher intensities of the field.

Theory

In this work, we treat mainly wormlike flexibility and compare the results with those obtained for segmental flexibility. For wormlike flexible macromolecules, we shall use the model proposed by Hagerman and Zimm.[39]

In a previous paper,[14] we presented a description of the birefringence of segmentally flexible macromolecules, which is a straightforward adaptation of the general theory of birefringence. In that work, we particularized the case in which the subunits comprising the macromolecule had a cylindrically symmetric polarizability for a general chain consisting of a certain number of segments. When such a chain contains several subunits, different types of flexibility can be reproduced. The two extreme cases named above can also be modeled: broken rod, if flexibility is concentrated at a single place, and wormlike macromolecule if flexibility is distributed along the chain being modeled. The same results can be used for models with N subunits, although in the above paper they were applied to the case of a chain with two subunits (the simplest case of segmental flexibility). Now, we recall some of them, particularizing for the case of N subunits.

Orientation and Birefringence. The excess birefringence of a macromolecular solution with respect to that of the pure solvent, Δn, is given in general by

$$\Delta n = K_n \nu \Delta\Gamma \tag{1}$$

In this equation, $K_n = 2\pi(n^2 + 2)^2/9n$, n being the refractive index. In eq 1, $\nu = cN_A/M$, with c and M being the weight concentration and molecular weight of the macromolecular solute. Also in eq 1 appears $\Delta\Gamma$, which is the anisotropy of the mean optical-polarizability tensor, $\langle\Gamma\rangle$, of the macromolecule, expressed as

$$\Delta\Gamma = \langle\Gamma_{zz}\rangle - \langle\Gamma_{xx}\rangle \tag{2}$$

We now particularize to the case in which the subunits comprising the macromolecule have a cylindrically symmetric polarizability. For a general chain consisting of N segments whose optical properties are cylindrically symmetric, the mean polarizability tensor is

$$\langle\Gamma\rangle = \langle\sum_{i=1}^{N}\gamma_{\perp,i}\rangle\,\mathbf{I} + \langle\sum_{i=1}^{N}\hat{\mathbf{Q}}_i\hat{\mathbf{Q}}_i(\gamma_{\parallel} - \gamma_{\perp})_i\rangle \tag{3}$$

In eq 3, $\mathbf{I}$ is the identity tensor, and $\gamma_{\parallel,i}$ and $\gamma_{\perp,i}$ are the main components of the polarizability tensor of the ith segment, along the segment axis and perpendicular to it, respectively. $\hat{\mathbf{Q}}_i$ is an unitary vector along the segment axis.

The *sat* subindex indicates that the corresponding quantity is saturated, reaching a limiting value in very high fields. It is useful to define a normalized birefringence by referring to the limiting value:

$$\Delta n^* \equiv \frac{\Delta n}{\Delta n_{\mathrm{sat}}} \tag{4}$$

From former equations[14] we obtain, for N subunits:

$$\Delta n^* = \sum_{i=1}^{N} x_i \langle P_2(\cos\theta_i)\rangle \tag{5}$$

In eq 5, $P_2(\cos\theta_i)$ is the second Legendre polynomial of the angle θ_i defined as $P_2(\cos\theta) = (3\cos^2\theta - 1)/2$. Also in eq 5 appears x_i, which is the fraction

$$x_i = \frac{(\gamma_{\parallel} - \gamma_{\perp})_i}{\sum_{i=1}^{N_s}(\gamma_{\parallel} - \gamma_{\perp})_i} \tag{6}$$

One particular case of interest is when all the subunits have a similar elongated structure of identical composition (for instance, helices) and only differ in length. In this case, we may take $(\gamma_{\parallel} - \gamma_{\perp})_i \propto L_i$, where L_i is the subunit length.

Deformation in the Presence of the Field. The gyration tensor is defined as

$$\langle \mathbf{G} \rangle = \left\langle \frac{1}{m}\int_V \mathbf{ss}\,\rho(\mathbf{s})\,d\tau \right\rangle \tag{7}$$

For a flexible particle, the average $\langle ... \rangle$ must be carried out over all the conformations that the particle may adopt. In eq 7, for an instantaneous conformation, **s** is the position vector of a point within the particle with respect to its instantaneous center of mass, and **ss** is the tensor with Cartesian components $\mathbf{ss}_{\alpha\beta} = s_\alpha s_\beta$, where $\alpha, \beta = x, y, z$.

When a situation corresponding to the absence of external agents is considered, a particle of arbitrary shape can have any orientation in space and any possible conformation (as determined by a set of values of the internal variables). In other words, independently of the rigidity or flexibility of the structure, the orientation of the particle and that of any of its subunits is uniformly random. As a consequence, the gyration tensor is extremely simple: it takes a diagonal form, with diagonal components equal to one-third of the squared radius of gyration, $\langle s^2\rangle_0$:

$$\langle \mathbf{G} \rangle_0 = \langle G \rangle_{\alpha\alpha,0}\mathbf{I} \tag{8}$$

$$\langle G \rangle_{\alpha\alpha,0} = 1/3\,\langle s^2 \rangle_0 \tag{9}$$

$$\langle s^2 \rangle_0 = \sum f_i(\langle d_i^2 \rangle_0 + s_i^2) \tag{10}$$

$\langle ... \rangle_0$ indicates a mean (both orientational and conformational) in the absence of field. Subscript 0 indicates the absence of field. d_i is the (instantaneous) value of the distance form the center, c_i, of subunit i to the center of mass and $f_i = m_i/\Sigma m_i$ is the mass fraction of that subunit.

Under the action of the field, the molecule is deformed and its average dimensions are modified. The change in the radius of gyration may be expressed in terms of a deformation ratio[40]

$$\delta^2 = \frac{\langle s^2 \rangle - \langle s^2 \rangle_0}{\langle s^2 \rangle_0} \tag{11}$$

In eq 11, δ^2 is the change in $\langle s^2\rangle$ relative to its unperturbed value.

Similarly, this definition can be extended to all the diagonal components of the gyration tensor, changes in which are expressed with respect to the unperturbed value of the diagonal components, so that

$$\delta^2_{\alpha\alpha} = \frac{\langle \mathrm{G} \rangle_{\alpha\alpha} - 1/3\langle s^2 \rangle_0}{1/3\langle \mathrm{s}^2 \rangle_0} \tag{12}$$

It follows from eqs 11 and 12 that

$$\delta^2 = 1/3(\delta_{xx}{}^2 + \delta_{yy}{}^2 + \delta_{zz}{}^2) \tag{13}$$

In most cases of practical interest, the external agent acts along a given direction (say, axis z), and the perpendicular directions (axes x and y) are equivalent, for example, orientation in an electric field or shear or axial elongational flow. In those circumstances, $\delta_{xx}{}^2 = \delta_{yy}{}^2$.

If the subunits were replaced by pointlike elements with masses m_i positioned at the c_i's, the components of the gyration tensor would be $\langle G'_{\alpha\alpha}\rangle = \Sigma f_i \langle d_{i,\alpha}{}^2\rangle$ and $\langle s'^2\rangle = \Sigma f_i \langle d_i{}^2\rangle$, with $\langle s'^2\rangle = \langle G'_{xx}\rangle + \langle G'_{yy}\rangle + \langle G'_{zz}\rangle$. The sums are over the N_s subunits. The deformation parameters would be given by eqs 11 and 12 with the primed values $\langle G'_{\alpha\alpha}\rangle$ and $\langle s'^2\rangle$.

Carrasco et al.[14] showed that for a multisubunit structure, the gyration tensor and, as a consequence, $\delta_{\alpha\alpha}{}^2$ and δ^2 can be expressed in terms of two types of contribution, one based on the distances of the subunits to the center of mass and another on the gyration tensor of the subunits. For the calculation of these magnitudes, we recall some equations presented in the same paper and we rewrite them in a form suitable for our purposes. Concretely, when the model is based on axially symmetric subunits we can write

$$\delta_{xx}{}^2 = \frac{\delta'_{xx}{}^2\langle s'^2\rangle_0 + \sum f_i \langle P_2(\cos\theta_i)\rangle (G_i^{\perp} - G_i^{\parallel})}{\langle s'^2\rangle_0 + \sum f_i(2G_i^{\perp} + G_i^{\parallel})} \tag{14}$$

$$\delta_{zz}{}^2 = \frac{\delta'_{zz}{}^2\langle s'^2\rangle_0 - 2\sum f_i \langle P_2(\cos\theta_i)\rangle (G_i^{\perp} - G_i^{\parallel})}{\langle s'^2\rangle_0 + \sum f_i(2G_i^{\perp} + G_i^{\parallel})} \tag{15}$$

$$\delta^2 = \frac{\delta'^2\langle s'^2\rangle_0}{\langle s'^2\rangle_0 + \sum f_i(2G_i^{\perp} + G_i^{\parallel})} \tag{16}$$

When all the subunits of the model are equal, then $G_i^{\perp} = G^{\perp}$ and $G_i^{\parallel} = G^{\parallel}$, and further simplification is possible. If we recall the definition of Δn^* given by eq 5, we can write

$$\delta_{xx}{}^2 = \frac{\delta'_{xx}{}^2\langle s'^2\rangle_0 + \Delta n^*(G^{\perp} - G^{\parallel})}{\langle s'^2\rangle_0 + (2G^{\perp} + G^{\parallel})} \tag{17}$$

$$\delta_{zz}{}^2 = \frac{\delta'_{zz}{}^2\langle s'^2\rangle_0 - 2\Delta n^*(G^{\perp} - G^{\parallel})}{\langle s'^2\rangle_0 + (2G^{\perp} + G^{\parallel})} \tag{18}$$

$$\delta^2 = \frac{\delta'^2\langle s'^2\rangle_0}{\langle s'^2\rangle_0 + (2G^{\perp} + G^{\parallel})} \tag{19}$$

In this case, the effect of the field in the deformation of the whole molecule (as expressed by eqs 17−19) can be calculated by means of different variables. Deformation and orientation are addressed by $\delta'_{\alpha\alpha}{}^2$, δ'^2, and Δn^*, which are independent not only of the shape and size of the subunits but also of the overall size of the molecule and of the number of subunits used to model it. The overall size and shape of the molecule is taken into account through $\langle s'^2\rangle_0$, but, according to its definition, its value is independent of the field and the characteristics of the subunits. Finally, the shape and size of the subunits are included by means of $G^{\perp}$ and $G^{\parallel}$. The most illustrative results for our purposes are those which refer to $\delta'_{\alpha\alpha}{}^2$, δ'^2, and Δn^*. These results can be easily transferred to a given particular case.

Scattering. The average size of the macromolecule, as determined by the radius of gyration, is often obtained from low-angle scattering of light or other electromagnetic radiation. When the macromolecule is deformed in an electric field, it may be possible to obtain the components of the gyration tensor from scattering with various geometries. Instrumental and theoretical aspects of the technique of electric field light scattering have been described in the literature.[26,27]

The dependence of scattered intensity on the scattering direction is represented by the scattering form factor, P(**q**):

$$\mathrm{P}(\mathbf{q}) = \left\langle \mathbf{Re}\left[\frac{1}{m^2}\int_V \int_V \exp(-\mathbf{iq}\cdot\mathbf{r}_{12})\,\rho(\mathbf{r}_1)\rho(\mathbf{r}_2)\,\mathrm{d}\tau_1\mathrm{d}\tau_2\right]\right\rangle \quad (20)$$

In eq 20, **q** is the scattering vector with modulus $q = (4\pi/\lambda)\sin(\theta_s/2)$, where λ is the radiation wavelength and θ_s is the angle subtended by the scattering direction and the prolongation of the incident beam. The integration extends to all the pairs of points within the particle, with position vectors $\mathbf{r}_1$ and $\mathbf{r}_2$. In eq 20, $\mathbf{r}_{12} = \mathbf{r}_2 - \mathbf{r}_1$.

If we take the real part in eq 20 and assume low-angle scattering so that $\mathbf{q}\cdot\mathbf{r}_{12}$ is small for every pair of points, then, taking the linear term in a series expansion on powers of $\mathbf{q}\cdot\mathbf{r}_{12}$ and bearing in mind the second definition of the gyration tensor, we can write

$$\mathrm{P}(\mathbf{q}) = 1 - \sum_\alpha \sum_\beta q_\alpha q_\beta \langle G\rangle_{\alpha\beta} \quad (21)$$

This expression was presented in an earlier work[24] for the special case of a chain of pointlike scatterers.

A particular situation of interest is that corresponding to an experimental setup in which scattering is observed in the (x, y) plane of the lab-fixed system of coordinates, x is the direction of the incident beam. For low angle scattering, **q** is approximately perpendicular to x, almost pointing in the y direction. Then, $\mathbf{q} \approx (0, q, 0)$ in the laboratory coordinates, and

$$\mathrm{P}(\mathbf{q}) \approx 1 - q^2\langle G\rangle_{yy} \quad (22)$$

Similarly, if the scattering is observed in a vertical plane (x, z), with x being the direction of the incident beam, P(**q**) would again be given by eq 22 substituting $\langle G\rangle_{yy}$ by $\langle G\rangle_{zz}$.

Following eq 22, the change in the scattering form factor can be written as

$$\frac{\mathrm{P}_0(\mathbf{q}) - \mathrm{P}(\mathbf{q})}{1 - \mathrm{P}_0(\mathbf{q})} \approx \frac{\langle \mathrm{G}\rangle_{\beta\beta} - \langle \mathrm{G}\rangle_{\beta\beta,0}}{\langle \mathrm{G}\rangle_{\beta\beta,0}} = \delta_{\beta\beta}{}^2 \quad (23)$$

As shown by eq 23, the change in the scattering form factor is independent of the scattering angle. We recall that β is the direction perpendicular to the incident beam in the scattering plane. Thus, changing the mutual orientation of the scattering plane and the electric field, the electric field light-scattering experiment could provide the values for all the $\delta_{\alpha\alpha}{}^2$ and δ^2. As will become apparent in the presentation of the results, the greatest deformation is in the direction of the field and will be measured by applying the field in the scattering plane, perpendicular to the incident beam.

Models and Methods

In this paper, we study the steady-state properties of wormlike macromolecules under an external electric field. For this, we first need a model that reproduces wormlike flexibility, to which end we present a methodology for constructing models of semiflexible macromolecules based on a discrete number of subunits. This general method can be used for segmental or wormlike flexibility. For a given model, the steady state reached under an electric field can be simulated using Monte Carlo techniques, simply defining the two contributions to the potential energy of the molecule, V, in an electric field.

$$V = V_{\mathrm{int}} + V_{\mathrm{elect}} \quad (24)$$

In this equation, V_{int} refers to the internal potential energy, defined by the characteristics of the model, and V_{elect} gives the interaction of the model with the field. In the following section, we shall pay attention to these different aspects.

Modeling Semiflexible Macromolecules. The term V_{int} of eq 24 is the internal energy associated to the deformation of the macromolecule, that is, to its departure from the most stable configuration. Our models are chains made up of $N + 1$ pointlike elements. Their connectors define N axially symmetric subunits and we assume that unitary vectors $\mathbf{u}_i$ ($i = 1$ to N) are aligned with the symmetry axis of each subunit. The instantaneous conformation of the particle is determined by a set of $N - 1$ angles, α_j, formed between two consecutive vectors. If $\alpha_{0,j}$ is the equilibrium value of these angles, the internal potential energy required for bending or deformation is given by

$$\frac{V_{\mathrm{int}}}{k_{\mathrm{B}}T} = \sum_{j=1}^{N-1} Q_j(\alpha_j - \alpha_{0,j})^2 \quad (25)$$

In this equation, $k_{\mathrm{B}}T$ is Boltzmann's factor and Q_j are the flexibility parameters, with $Q_j = 0$ for the completely flexible case and $Q_j \to \infty$ for the completely rigid one.

According to the values given to parameters Q_j and the number of subunits, different types of flexibility can be modeled. One extreme case is that whereby all Q_j have the same value and N is sufficiently high to provide a wormlike model (with limits $Q_j = \infty$ for a rigid chain and $Q_j = 0$ for a freely jointed chain).[39,41] Another extreme is defined when all $Q_{j\neq i} = \infty$ except one of them is different, $Q_i > \infty$. In this case, we have a model with two rigid arms and if the two arms are linear we have a broken-rod chain (BRC). Of course, the simplest broken-rod chain can also be modeled with two subunits and one single Q.[9,14,24]

Although in this work the equilibrium conformation is always a straight molecule (which is defined with all $\alpha_{0,j} = 0$), cases with one or several $\alpha_{0,j} \neq 0$ can be treated in the same way. Nonlinear molecules could also be modeled using this procedure.

Modeling Wormlike Flexibility. When no external agent deforms a wormlike macromolecule, it is accepted that the overall dimensions are given by the following equations:[42]

$$\langle r^2\rangle_0 = 2PL\left(1 - \frac{P}{L}(1 - \mathrm{e}^{-L/P})\right) \quad (26)$$

$$\langle s^2\rangle_0 = \frac{LP}{3} - P^2 + \frac{2P^3}{L}\left[1 - \frac{P}{L}(1 - \mathrm{e}^{-L/P})\right] \quad (27)$$

In these equations, $\langle r^2\rangle$ is the mean extreme-to-extreme square distance, $\langle s^2\rangle$ the mean radius of gyration, P the persistence length, and L the contour length. The subscript zero indicates the absence of any external deforming agent. When L/P is very small, or the macromolecules is rigid, eq 27 yields $s^2 = L^2/12$, which is the square radius of gyration of a infinitely thin cylinder of length L. For very large L/P, we have the flexible coil limits, $\langle r^2\rangle_0 = 2PL$ and $\langle s^2\rangle_0 = \langle r^2\rangle_0/6 = PL/3$. When defining

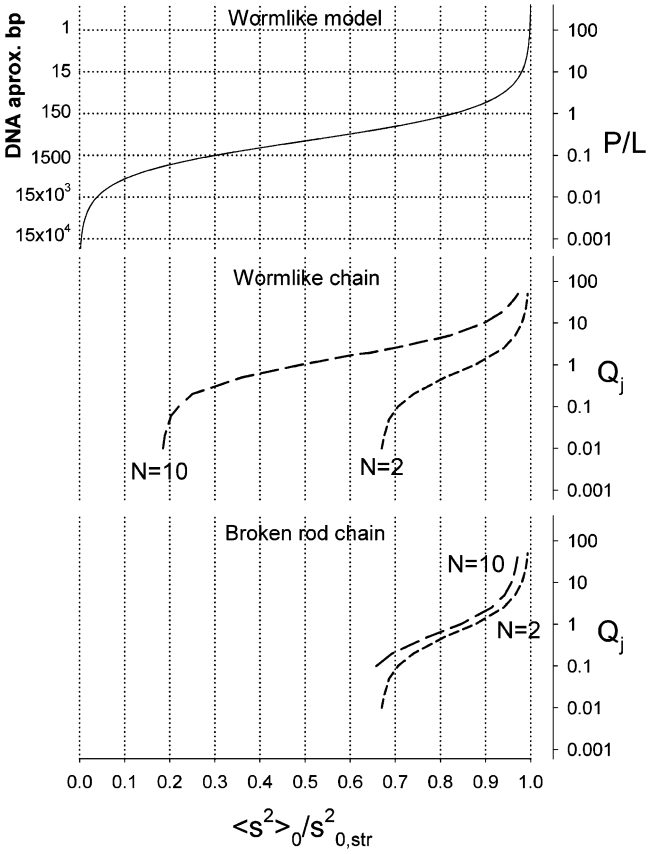

Figure 1. Relation between three different ways of characterizing flexibility (P/L, Q, and $\langle s^2\rangle_0/\langle s^2\rangle_{0,str}$) for wormlike model, wormlike chain, and broken-rod chain. The plot for the wormlike model was obtained from eq 27. For WLC and BRC, the computational results are presented. For illustrative purposes, the approximate correspondence between the number of base pairs of DNA with $P = 50$ nm and P/L is included.

flexibility/rigidity of a wormlike molecule, P should not be the only parameter used; indeed, the behavior depends not only on P but also on the contour length, L, of the molecule. We therefore use the ratio P/L to characterize the flexibility of a wormlike molecule.

Another way of assigning the degree of flexibility of a molecule is to use the ratio between the mean square radius of gyration of a model with certain flexibility and the value for a rigid straight one. In this work, we present results obtained for both wormlike and broken-rod chains; this way of presenting flexibility is very convenient because it has the advantage of being independent of the model (number of subunits and type of flexibility). Indeed, eq 27 gives $\langle s^2\rangle$ for a wormlike model, assuming an infinitely thin macromolecule (made of $N = \infty$ pointlike elements). As a consequence, when presented as $\langle s^2\rangle_0/\langle s^2\rangle_{0,str}$ these values are comparable with those obtained for chain models made up of several pointlike scatterers, which were represented by $\langle s'^2\rangle$ in eqs 14−19 (see above). From now on, we shall avoid the use of the prime symbol ($'$) in all the calculated parameters.

When using linear chain models of several subunits, flexibility is discretely localized in the hinges of the chain. Flexibility in these chain models is defined by parameters Q_j (see eq 25). In Figure 1, we present plots to illustrate the correspondence between the three parameters that are used to define flexibility: P/L, Q, and $\langle s^2\rangle_0/\langle s^2\rangle_{0,str}$.

Figure 1 is also useful for delimiting the ranges of flexibility. From the plot of P/L versus $\langle s^2\rangle_0/\langle s^2\rangle_{0,str}$ three different situations can easily be delimited: when $\langle s^2\rangle_0/\langle s^2\rangle_{0,str}$ is very low, the flexibility is that exhibited by the random coil. At the other extreme, when $\langle s^2\rangle_0/\langle s^2\rangle_{0,str}$ is close to 1 we are clearly dealing with a rigid rod. Between these two limits, the flexibility must be wormlike.

Figure 1 shows some results for two linear chain models of a different number of subunits ($N = 10$ and $N = 2$). In this paper, we study the wormlike chain (WLC), and for comparison, the broken rod. In the first case, all the angle springs have the same flexibility to a degree that can vary. In the second case all the angle springs, except one of them, must be very stiff. From the computational point of view, it is very important to define the right characteristics of the model to be simulated. For example, we have found that $N = 10$ is a suitable number of subunits to represent wormlike flexibility within a wide range of P/L. Although the same $N = 10$ could be used to represent the broken rod, a very similar and much simpler representation is obtained with $N = 2$. The small differences between both (see broken-rod chain in Figure 1) can be attributed to certain simplifications of the simulation technique. For these models, the degree of flexibility is defined by the set of parameter Q_j (see eq 25) using the same values as those used in previous works.[14−16] For each individual hinge, the range goes from 50 (this is our rigid limit) to 0 for total flexibility. For $Q_j = 50$, a certain variation in the angle is allowed (Q_j could be as high as desired but increases the computational cost). This explains differences for BRC between $N = 10$ and $N = 2$. According to Figure 1, the overall dimensions of a given macromolecule, withing certain limits, can be described computationally by both WLC and BRC.

For properties which only depend on the overall dimensions, we find the representation proposed in Figure 1 to be very useful. For example, it allows us to choose the most suitable model to represent DNA, because the expected values of P/L for DNA molecules of different lengths can be readily obtained. As an illustration, Figure 1 has been provided with an axis with the approximate number of base pairs (bp) corresponding to some values of P/L (we have assumed that $P = 50$ nm and that each additional base pair increases L by 0.34 nm). For instance, a DNA with approximately 1500 base pairs (nearly 10^6 Da) can be represented as a wormlike chain with $N = 10$ segments and $Q_j = 0.5$.

By referring to the information given in Figure 1, we see that long DNA molecules have a very low P/L ratio, and so a very flexible model is needed to describe its behavior. This should help clarify the following point, whereby flexible models (e.g., Rouse−Zimm model[21]) were used to describe experimental results for long DNA samples, which was considered a somewhat surprising finding. However, Figure 1 shows clearly that for long DNA molecules only flexible models can explain the results.

In addition, simple but interesting information can be obtained from the type of representation used in Figure 1. When the ratio $\langle s^2\rangle_0/\langle s^2\rangle_{0,str}$ is lower than around 0.65 the type of flexibility found in a linear molecule cannot be obtained from a trumbbell, and a certain degree of wormlike flexibility must be contained in the macromolecule. This result agrees with the finding of Lewis et al.[43] concerning the limits existing in using a trumbbell as a model for DNA.

Semiflexible Macromolecules in an Electric Field. The second contribution to potential energy, according to eq 24, V_{elect}, gives the interaction energy of the molecule with the electric field and can be expressed as a sum of individual terms, $V_{elect,i}$, corresponding to the various subunits. These terms will depend

on the permanent dipoles, $\boldsymbol{\mu}_i$, if they exist, with a possible contribution from the induced dipoles determined by the electrical polarizabilities, ϵ_i. Their joint effect can be expressed in terms of the so-called alignment tensor:[4]

$$\boldsymbol{\chi}_i = (1/kT)^2 \boldsymbol{\mu}_i\boldsymbol{\mu}_i + (1/kT)\,\boldsymbol{\epsilon}_i \tag{28}$$

This vector will be additive if expressed in a common system of reference (the lab axes), so that for the full particle, $\boldsymbol{\chi} = \Sigma\boldsymbol{\chi}_i$. The interaction energy with an electric field, **E**, is given by $V_{\text{elect}} = \boldsymbol{\chi}\cdot\mathbf{E}$. When the subunits have revolution symmetry, we assume that $\boldsymbol{\mu}$ lies along the symmetry axis and that $\boldsymbol{\epsilon}$ has parallel and perpendicular components, $\epsilon^{||}$ and $\epsilon^{\perp}$. In this case, the interaction energy is reduced to a simple form, which contains the modules of the subunit dipoles, μ_i, and polarizability differences, $\epsilon_i^{||} - \epsilon_i^{\perp}$. This interaction energy depends on the angle, θ, subtended by the symmetry axis and the direction z of the electric field:

$$\frac{V_{\text{elect}}}{k_{\text{B}}T} = -\sum_{i=1}^{N}(a_i\cos\theta_i + b_i\cos^2\theta_i) \tag{29}$$

In this equation, $\cos\theta_i = (\mathbf{E}\cdot\mathbf{u}_i)/E$ and θ_i is the angle between the electric field and the symmetry axis. The parameters that describes the intensity of the molecule−field interaction are

$$a_i = \frac{\mu_i E}{k_{\text{B}}T} \tag{30}$$

$$b_i = \frac{(\epsilon_i^{||} - \epsilon_i^{\perp})E^2}{2k_{\text{B}}T} \tag{31}$$

When the permanent dipoles are nonzero, there are two possibilities for describing the disposition of the dipoles: head-to-head and head-to-tail. The parameter a_i is positive if μ_i is in the same direction as $\mathbf{u}_i$, and negative if it points in the opposite direction. In this work, we shall only study the second possibility, head-to-tail, which is the one that would be relevant for both broken-rod and wormlike chain models. The electric parameters are $b_i = 0$ for a purely permanent dipole moment (PER) and $a_i = 0$ for a purely induced moment (IND). To make the results independent of the number of subunits used to model a given macromolecule, the field strength must be expressed as $a^* = a \times N$ and $b^* = b \times N$.

Monte Carlo (MC) Simulation. To study the conformation of the macromolecule in the presence of an electric field and, more specifically, to evaluate the averages needed for the steady-state molecular shape and birefringence, we employ the same Monte Carlo (MC) procedure used by Iniesta and García de la Torre.[25] The total potential energy of the molecule is given by eq 24. V is a function of the set of polar angles of the arms in the laboratory system (θ_i and ϕ_i) which specify the orientations of the subunit vectors.

In this procedure, a new conformation of the particle is obtained from the previous one in the Monte Carlo step, by varying the orientation of the arms. This is done by adding random increments to $\cos\theta_i$ and ϕ_i whose maximum absolute values are $\Delta\cos\theta$ and $\Delta\phi$. The total energy is calculated for the new conformation, which is accepted if $V < V'$, where V' was the energy of the previous conformation. If this is not the case, a random number, ρ, uniformly distributed in (0,1) is generated. If $\rho > \exp[(V' - V)/kT]$, the new conformation is accepted; otherwise, it is rejected and the old conformation is counted once again.

For small values of the maximum increments $\Delta\cos\theta$ and $\Delta\phi$, the probability of acceptance is high although the conformational space is scanned slowly because of the small size of the simulation steps. For high increments, the probability of acceptance is low and so the scan speed is also slow. This is particularly true for high values of the electric field strength or the stiffness constant. When the number of subunits increases and so the number of contributions to the potential, the situation gets worse. We found it very difficult to obtain reproducible results for quasi-rigid models of $N = 10$ at low fields, because in this case, the two contributions to eq 24 are very different and V_{int} is much higher than V_{elect}. As a consequence, the number of conformations generated has to be very high to ensure that the conformational space is scanned correctly.

The typical values of $\Delta\cos\theta$ and $\Delta\phi$ we used in the simulations are 0.02 and 0.2, respectively. The number of conformations ranges from very few to several millions depending on the rigidity of the model and the intensity of the field. The set of conformations is divided into four subsets so that the statistical uncertainty of our final results is obtained from the standard deviation of the four subset averages.

Results

As we have explained, the application of an electric field of certain intensity for a sufficiently long period of time to reach steady state will affect flexible macromolecules in two main respects: their orientation according to the field and their deformation with respect to the field-free conformation. The first effect can be studied through changes in birefringence. The conformational changes (overall deformation) will be seen as changes in $\langle s^2\rangle$, and finally the changes in the components of $\langle\mathbf{G}\rangle$ will reflect both orientation and deformation of the semiflexible particle. These phenomena will be analyzed below.

Deformation Produced in the Molecule by an Electric Field. This is an interesting aspect that has received little attention. The response to the field involves orientation and deformation, both of which must depend on the internal structure of the molecule, for example, the type of dipole or type of flexibility.

To fully calculate gyration tensor and deformation, the size and shape of the subunits must be specified. However, we have found that the representation of $\delta_{\alpha\alpha}^2$ and δ^2 (as mentioned above, we avoid the use of ′) versus a^{*2} or $2b^*$ (equivalent to the square electric field) is representative of deformation (see eqs 17− 19 and comments below) and independent of the model (see above).

The results for $\delta_{\alpha\alpha}^2$ and δ^2 are shown in Figure 2. In this figure, we have chosen models with $\langle s^2\rangle_0/\langle s^2\rangle_{0,\text{str}} \cong 0.65$ for wormlike chain (WLC, $N = 10$) and broken-rod chain (BRC, $N = 2$) with permanent or induced dipoles.

The values shown in the plots of Figure 2 reflect the different behavior and sensitivity of $\langle G\rangle_{xx}$, $\langle G\rangle_{zz}$, and $\langle s^2\rangle$ and also their corresponding parameters, δ_{xx}^2, δ_{zz}^2, and δ^2, respect to the effect of field strength. For all the dipole types, $\langle G\rangle_{xx}$ goes from its field-free value, $\langle G\rangle_{xx,0}$, to zero, and correspondingly δ_{xx}^2 goes from 0 to −1. If the δ_{xx}^2 results are superimposed with a change of sign (not shown) on those of Δn^*, it immediately becomes clear that the trends of the points are quite similar. One difference between the wormlike and broken-rod models can be easily appreciated, since in the latter case even the numerical values coincide, which is not the case for the wormlike model. Therefore, the information provided by Δn^* and δ_{xx}^2 or, in other words, by electric birefringence and electric field light scattering

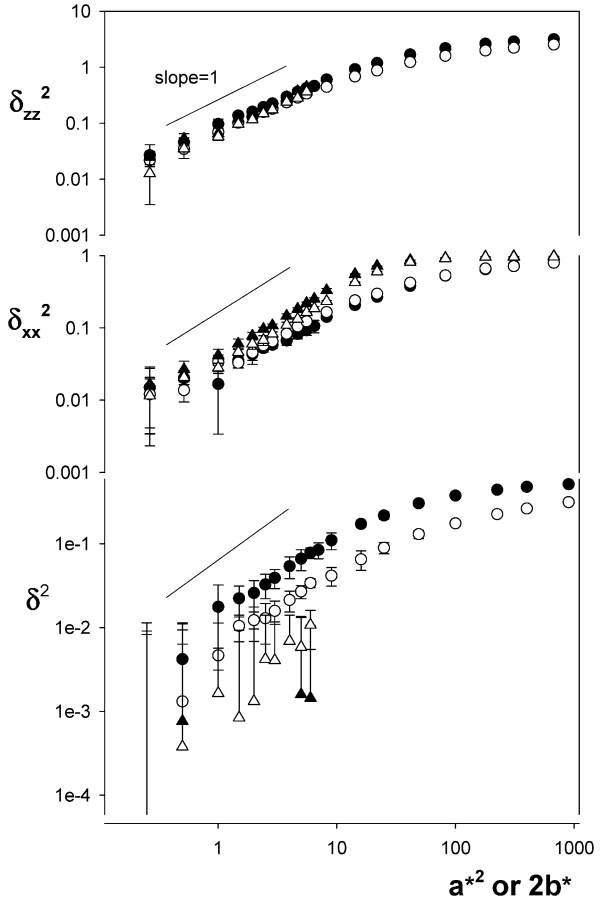

Figure 2. Plots of the deformation parameters δ_{zz}^2, δ_{xx}^2, and δ^2 (see text) versus intensity of the electric field for models with $\langle s^2\rangle_0/\langle s^2\rangle_{0,str} = 0.65$. Results for models with permanent dipoles are represented by circles and those with induced dipoles by triangles. White symbols are for WLC and black ones are for BRC.

with a horizontal scattering plane, is identical for BRC but different for WLC.

In Figure 2 we also show the plot corresponding to the δ_{zz}^2 component that is observed in electric field light scattering with a vertical scattering plane and the values of δ^2 corresponding to the expansion in the overall radius of gyration. The parameters δ_{zz}^2 and δ^2 behave differently, depending on the dipole type. If the dipole is permanent, an appreciable degree of expansion is observed, although the absolute values are moderate. In fact, remarkably high values of δ_{zz}^2 are reached at high fields for permanent dipoles, in contrast with the trend of the δ_{xx}^2 and Δn^*. When induced dipoles are simulated above a certain value of the electric field, no overall deformation is detected (statistical results are very poor). Again, this behavior is the same as that observed in the broken rod. The reasons are those explained in a previous paper[14] and will be illustrated when the distribution of angles is discussed.

Although the qualitative behavior is the same for segmentally flexible and wormlike macromolecules, in a permanent dipole, important quantitative differences are observed between both types of flexibility. If we look at δ^2, it is clear that deformation is lower for wormlike molecules. The parameter δ_{zz}^2 shows the same behavior. As a consequence, changes in δ^2 and δ_{zz}^2 with the field strength could be used to distinguish between segmental and wormlike flexibility.

Figure 2 also shows that, in the low field range, the three deformation parameters are proportional to E^2. This observation was already made for BRC[14] and now becomes clear for WLC, too. These results could be used, if the scattering technique were employed, to define the intensity of the field that limits the Kerr (or low field) region.

Although it is essential to study the change in the overall radius of gyration, characterization of the deformation process is improved if we look at the effects of the field on the distribution of angles, $P(\alpha_j)$, which can readily be obtained from the Monte Carlo simulations. Figure 3 shows histograms of this distribution of the central angle in a WLC ($N = 10$) with $\langle s^2\rangle_0/\langle s^2\rangle_{0,str} = 0.65$. We have checked (results not shown) that any other angle gives virtually the same results. In our previous paper devoted to BRC,[14] we showed histograms for $P(\alpha)$ which can be compared to the results shown in Figure 3 (the ratio $\langle s^2\rangle_0/\langle s^2\rangle_{0,str}$ is the same for both models).

In the absence of field, the fully flexible BRC with $\langle s^2\rangle_0/\langle s^2\rangle_{0,str} = 0.65$ shows a uniform distribution of angles[14] but the equivalent WLC does not show the same distribution uniformity. The reason is that $Q = 0$ for BRC while $Q_j \neq 0$ for WLC (in fact $Q_j = 1.8$). When field is applied to a particle with permanent dipoles, the particle is straightened by the field; conformations with a smaller α_j are favored and the peak in $P(\alpha_j)$ moves to the left. As a consequence, $\langle \cos \alpha_j\rangle$ should decrease below $\langle \cos \alpha_j\rangle_0$. However, the situation for induced dipoles is peculiar. For any value of b_i, the probability of any angle and that of its supplementary are characterized by Q_j (for $Q_j = 0$, both probabilities should be identical). In addition, the presence of the field should not change the radius of gyration. Indeed, this is shown when the field is low (results not shown). But there is a certain value of the field (very high for the WLC with $\langle s^2\rangle_0/\langle s^2\rangle_{0,str} = 0.65$) at which a bimodal distribution appears. Moreover, if the field is sufficiently high, this bimodal distribution becomes symmetrical. The reason is that at higher fields, the potential barrier that separates the conformations with $\alpha \approx 0$ and $\alpha \approx \pi$ is very high, so that during the simulation there are few transitions between one and the other extremes and the results are biased.

Steady-State Birefringence. Monte Carlo results for the steady-state birefringence of a wormlike macromolecule with $\langle s^2\rangle_0/\langle s^2\rangle_{0,str} \cong 0.65$ (equivalent to the fully flexible BRC) and permanent or induced dipoles are shown in Figure 4. The electric birefringence of the two-subunit particle was already studied in previous studies,[14,25] but we have also included results for this type of particle in Figure 4. For reference purposes, data of a rigid model obtained using the same simulation technique are also included.

When $\Delta n^*(0)$ is plotted versus a^{*2} or $2b^*$, we must distinguish between the behavior at low fields and that at medium or high fields. The first is described by the Kerr law and implies a linear dependence of $\Delta n^*(0)$ on E^2. If we represent $\Delta n^*(0)$ versus a^{*2} or $2b^*$ in the Kerr region in a log−log plot, the result is a linear dependence with a slope of 1. Figure 4 shows this behavior for wormlike chains and broken-rod chains. In this figure, we see that the strength of the field at which the departure from linearity is observed (limit of the Kerr region) is not significantly sensitive to the type of dipole or the degree and type of flexibility. Finally, this figure illustrates the difficulties involved in obtaining results with good statistical quality when the field is low and how this difficulty is enhanced for rigid models.

In the region of medium and high field strength, we find that WLC and BRC show similar qualitative behavior, although some significant differences appear from a quantitative point of view. For molecules with the same flexibility (identical $\langle s^2\rangle_0/\langle s^2\rangle_{0,str}$), steady-state birefringence is lower in the case of

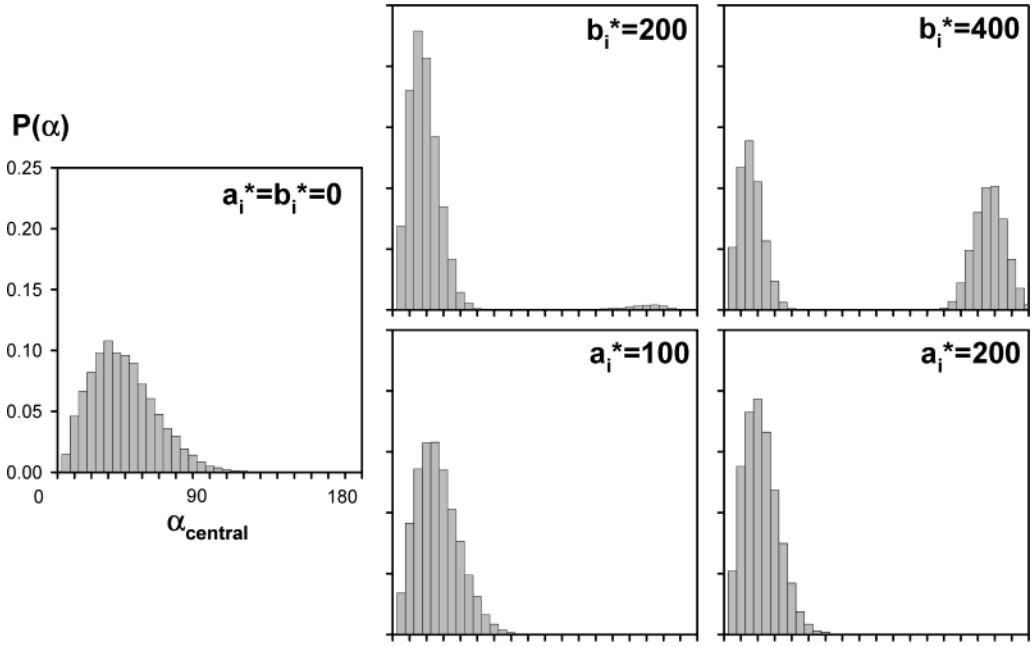

Figure 3. Angle distribution for a wormlike chain with $N = 10$. These results refer to the central angle although no significant difference is observed for a different angle. We have included results in the absence of an electric field ($a_i^* = b_i^* = 0$) and two values of a_i^* and b_i^* in the region of strong−very strong fields. In the region of low and medium intensities of the field, no appreciable deviation is observed with respect to the field free distribution.

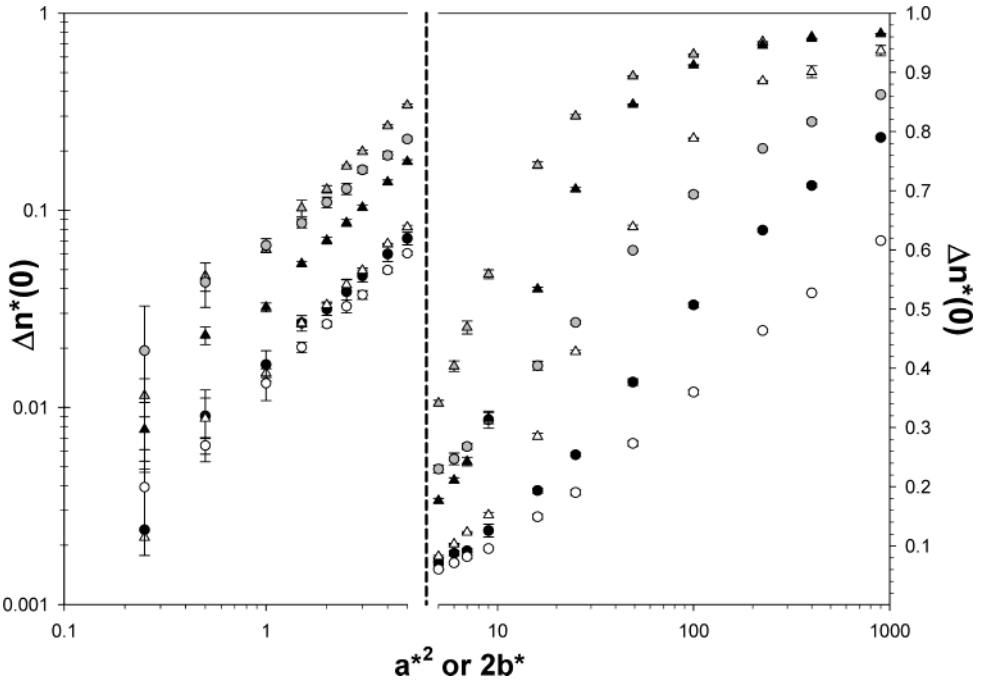

Figure 4. Steady-state value of reduced birefringence, $\Delta n^*(0)$, versus field strength. Two different scales have been used for the low field region (y axis is in logarithmic scale) and medium−high field region (y axis is in linear scale). Model flexibility is defined by $\langle s^2\rangle_0/\langle s^2\rangle_{0,str} = 0.65$. Results for models with permanent dipoles are represented by circles and with induced dipoles by triangles. White symbols are for WLC and black ones are for BRC. For reference purposes, data for a rigid model (grey symbols) obtained using the same simulation technique are included.

wormlike flexibility at the same field strength. The broken-rod chain reaches saturation at lower fields. This behavior is common to permanent and induced dipoles but is more pronounced in the latter. Finally, simulating molecules with a different degree of flexibility (results not shown) leads us to another conclusion: the dependence of the model on the degree of flexibility is greater for wormlike than for segmentally flexible macromolecules.

Summary

A model of $N + 1$ pointlike elements whose connectors define N axially symmetric subunits is able to describe segmentally flexible and wormlike macromolecules. We simply need to choose the right value of N. In this work, we use the flexibility parameter $\langle s^2\rangle_0/\langle s^2\rangle_{0,str}$ and we describe its relationship with P/L for wormlike molecules and with Q for segmentally flexible

molecules. A Monte Carlo computer simulation characterizes the effect of a steady-state electric field on the orientation and deformation of molecules with permanent and induced dipoles. Using this technique, the differences between the behavior of a broken rod and a wormlike chain become evident. These differences are generally quantitative, although significant enough to be used to obtain information about the internal structure of a given macromolecule.

Acknowledgment. This work has been funded by grant BQU2000-0229 from the Direccion General de Enseñanza Superior e Investigación Científica (M.E.C.).

References and Notes

(1) Frederick, E.; Houssier, C. *Electric Dichroism and Electric Birefringence*; Clarendon Press: Oxford, 1973.
(2) Riande, E.; Saiz, E. *Dipole Moments and Birefringence of Polymers*; Prentice Hall: Englewood Cliffs, NJ, 1992.
(3) Holcomb, D. N.; Tinoco, I. J. *J. Phys. Chem.* **1963**, *67*, 2691.
(4) Wegener, R. M.; Dowben, R. M.; Koester, V. J. *J. Chem. Phys.* **1979**, *70*, 622.
(5) García de la Torre, J.; Bloomfield, V. A. *Quart. Rev. Biophys.* **1981**, *14*, 81.
(6) García, de la Torre, J. Rotational diffusion coefficients. In *Molecular Electro-optics*; Krause, S., Ed.; Plenum Publishing Corporation: New York, 1981.
(7) García, de la Torre, J. Hydroynamic Properties of Macromolecular Assemblies. In *Dynamic Properties of Macromolecular Assemblies*; Harding, S., Rowe, A., Eds.; The Royal Society of Chemistry: Cambridge, 1989.
(8) Harvey, S. C.; Cheung, H. Myosin Flexibility. In *Cell and Muscle Motility* Vol. 2; Dowben, R. M., Shay, J. W., Eds.; Plenum: New York, 1982; p 279−302.
(9) Iniesta, A.; Díaz, F. G.; García de la Torre, J. *Biophys. J.* **1988**, *54*, 269.
(10) Matsumoto, T.; Nishioka, N.; Teramoto, A.; Fujita, H. *Macromolecules* **1975**, *7*, 824.
(11) Muroaga, Y.; Tagawa, H.; Hiragi, Y.; Ueki, T.; Kataoka, M.; Izuni, Y.; Aneniya, Y. *Macromolecules* **1988**, *21*, 2760.
(12) García de la Torre, J.; Bloomfield, V. A. *Biochemistry* **1980**, *19*, 5118.
(13) Burton, D. F. Structure and function of antibodies. In *Molecular Genetics of Immunoglobulin*; Calabi F., Neuberger, M. S., Eds.; Elsevier: Amsterdam, 1987; p 1−50.
(14) Carrasco, B.; Díaz, F. G.; López Martínez, M. C.; García de la Torre, J. *J. Phys. Chem.* **1999**, *103*, 7822.
(15) Díaz, F. G.; Carrasco, B.; López Martínez, M.; García de la Torre, J. *J. Phys. Chem.* **2000**, *104*, 12339.
(16) Pérez Sánchez, H. E.; García de la Torre, J.; Díaz Baños, F. G. *J. Phys. Chem. B* **2002**, *106*, 6754.
(17) Blommfield, V. A.; Crothers, D. M.; Tinoco, I., Jr. *Physical Chemistry of Nucleic Acids*; Harper & Row Publishers: New York, 1974.
(18) Blommfield, V. A.; Crothers, D. M.; Tinoco, I., Jr. *Nucleic Acids: Structures, Properties and Functions*; University Science Books: Sausalito, CA, 2000.
(19) Hagerman, P. J. *Annu. Rev. Biophys. Biomol. Struct.* **1997**, *26*, 139.
(20) Bertolotto, J. A.; Campo, M. G.; Roston, G. B.; Ascheri, M. E. *Colloids Surf., A* **2002**, *203*, 167.
(21) Lewis, R. J.; Pecora, R. *Macromolecules* **1986**, *19*, 2074.
(22) Lewis, R. J.; Allison, S. A.; Eden, D.; Pecora, R. *J. Chem. Phys.* **1988**, *89*, 2490.
(23) Mellado, P.; García de la Torre, J. *Biopolymers* **1982**, *21*, 1857.
(24) Navarro, S.; Carrasco, B.; López Martínez, M. C.; García de la Torre, J. *J. Polym. Sci., Part B: Polym. Phys.* **1997**, *35*, 689.
(25) Iniesta, A.; García de la Torre, J. *J. Chem. Phys.* **1989**, *90*, 5190.
(26) Jennings, B. R. Light scattering in electric fields. In *Molecular Electro-optics*; Krause, S., Ed.; Plenum Publishing Corporation: New York, 1981.
(27) Khanarian, G.; Stein, R. S. *Macromolecules* **1987**, *20*, 2858.
(28) Heller, W. *J. Chem. Phys.* **1982**, *76*, 69−74.
(29) Link, A.; Springer, J. *Macromolecules* **1993**, *26*, 464.
(30) Harvey, S. C.; Mellado, P.; García de la Torre, J. *J. Chem. Phys.* **1983**, *78*, 2081.
(31) García de la Torre, J. *Eur. Biophys. J.* **1994**, *23*, 307.
(32) Yamaoka, K.; Fukudome, K. *J. Phys. Chem.* **1988**, *92*, 4994.
(33) Stellwagen, N. C. *Biopolymers* **1981**, *20*, 399.
(34) Stellwagen, N. C.; Bossi, A.; Gelfi, C.; Righetti, P. G. *Electrophoresis* **2001**, *22*, 4311.
(35) Redowicz, M. J.; Korn, E. D.; Rau, D. C. *J. Biol. Chem.* **1996**, *271*, 12401.
(36) Porschke, D.; Creminon, C.; Cousin, X.; Bon, C.; Sussman, J.; Silman, I. *Biophys. J.* **1996**, *70*, 1603.
(37) Zacher, R. A. *J. Chem. Phys.* **1990**, *93*, 1325.
(38) Stellwagen, N. C. *Biopolymers* **1991**, *31*, 1651.
(39) Hagerman, P. J.; Zimm B. H. *Biopolymers* **1981**, *20*, 1481.
(40) López Cascales, J. J.; Navarro, S.; García de la Torre, J. *Macromolecules* **1992**, *25*, 3574.
(41) Allison, S. A. *Macromolecules* **1986**, *19*, 118.
(42) Yamakawa, H. *Modern Theory of Polymer solutions*; Harper and Row: New York, 1971.
(43) Lewis, R. J.; Pecora, R.; Eden, D. *Macromolecules* **1986**, *19*, 134.